IEICE TRANS. COMMUN., VOL.E90–B, NO.4 APRIL 2007

PAPER

# Frequency-Domain Adaptive Antenna Array for Multi-Code MC-CDMA

Osamu NAKAMURA[†a)], Shinsuke TAKAOKA[†], Eisuke KUDOH[†], *and* Fumiyuki ADACHI[†], *Members*

**SUMMARY** MC-CDMA is an attractive multi-access method for the next generation high-speed mobile communication systems. The uplink transmission performance is limited by the multi-access interference (MAI) from other users since all users share the same bandwidth. Adaptive antenna array can be used to suppress the MAI and to improve the uplink transmission performance. In this paper, we propose a frequency-domain adaptive antenna array for multi-code MC-CDMA. The proposed frequency-domain adaptive antenna array uses a simple normalized LMS (NLMS) algorithm. Although the NLMS algorithm is used, very fast weight convergence within one MC-CDMA symbol duration is achieved since the weight updating is possible as many times as the number of subcarriers within one MC-CDMA symbol duration.

***key words:*** *MC-CDMA, adaptive antenna array, adaptive algorithm, frequency-domain*

## 1. Introduction

High speed and high quality data services are strongly demanded for the next generation mobile communication systems. Since the mobile channel is composed of many propagation paths with different time delays, the channel becomes severely frequency-selective, which degrades the transmission performance [1]. Recently, orthogonal frequency division multiple access (OFDMA) and multicarrier code division multiple access (MC-CDMA) have been attracting attention as promising candidates for the next generation systems, because of their robustness against the frequency-selectivity of the channel [2]–[4].

The uplink (mobile-to-base) transmission performance is limited by the multi-access interference (MAI). Adaptive antenna array is an attractive technique for suppressing the MAI [5]. Adaptive antenna array for OFDMA and MC-CDMA can be classified into post-FFT type [6], [7] and pre-FFT type [8]. In this paper, we propose frequency-domain adaptive antenna array, which falls in the post-FFT type, for the orthogonal multi-code MC-CDMA uplink transmission. The proposed frequency-domain adaptive antenna array uses the desired signal after array combining as the reference signal. This idea is also used in Ref. [9]. (However, the access scheme considered in Ref. [9] is direct sequence code division multiple access (DS-CDMA)). The proposed adaptive antenna array in this paper is designed to minimize the average interference power. This allows us to use the same array weight for all subcarriers and hence, the array weights can be updated, in one OFDM symbol duration, as many times as the number of subcarriers. Because of this, a very fast weight convergence can be achieved although a simple normalized least mean square (NLMS) algorithm is used. The adaptive antenna array studied in Ref. [8] is pre-FFT type. The time-domain reference signal generation and array weight updating at every sampling time are necessary for achieving fast array weight convergence. On the other hand, our proposed method uses the frequency-domain reference signal. In this paper, the optimum array weight is theoretically derived based on the Lagrange multipliers method under the weight constraint. Also derived is the equalization weight when frequency-domain equalization (FDE) based on the minimum mean square error (MMSE) criterion is used after array combining.

The remainder of this paper is organized as follows. Section 2 describes the multi-code MC-CDMA uplink with frequency-domain adaptive antenna array. The frequency-domain array weight updating algorithm is presented in Sect. 3. Section 4 gives the bit error rate (BER) analysis. The simulation and numerical results are presented in Sect. 5. Finally, Sect. 6 concludes the paper.

## 2. Multi-Code MC-CDMA with Frequency-Domain Adaptive Antenna Array

### 2.1 Transmit Signal

We assume that $U$ users are transmitting their MC-CDMA signals with $N_c$ subcarriers. $SF$ and $C$ denote the spreading factor and the code multiplexing order, respectively. Figure 1 illustrates the $u$-th user multi-code MC-CDMA transmitter structure. The binary data sequence is transformed into a data-modulated symbol sequence and is serial-to-parallel (S/P) converted into $C$ streams $\{d_{u,c}(i); i=0\sim N_c/SF-1\}$, $c=0\sim C-1$. Each stream is spread by orthogonal spreading code $\{c_{u,c}(k); k=0\sim SF-1\}$, $c=0\sim C-1$. The $C$ spread sequences are then combined and further multiplied by a

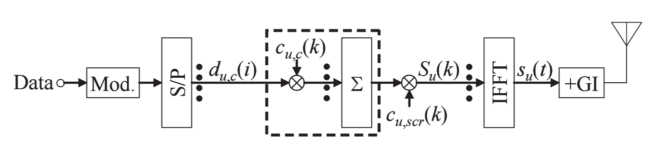


**Fig. 1** Transmitter structure of the $u$-th user.

Manuscript received March 28, 2006.
Manuscript revised July 19, 2006.

[†]The authors are with the Department of Electrical and Communications Engineering, Tohoku University, Sendai-shi, 980-8579 Japan.
a) E-mail: osamu.nakamura@sharp.co.jp

DOI: 10.1093/ietcom/e90–b.4.918

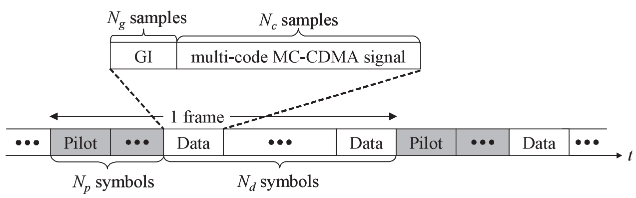


**Fig. 2** Frame structure.

scramble sequence $\{c_{u,scr}(k);\ k{=}0{\sim}N_c-1\}$. The code-multiplexed chip sequence is divided into a sequence of chip blocks of $N_c$ chips. $N_c$-point IFFT is applied to each $N_c$-chip block to generate the MC-CDMA signal. The MC-CDMA signal after the insertion of $N_g$-sample guard interval (GI) can be expressed using the equivalent lowpass representation as

$$s_u(t)=\sum_{k=0}^{N_c-1}S_u(k)\exp\left(j2\pi k\frac{t}{N_c}\right)\quad\text{for } t=-N_g{\sim}N_c-1,\quad(1)$$

where

$$S_u(k)=\sqrt{\frac{2P_u}{SF}}\sum_{c=0}^{C-1}c_{u,c}(k \bmod SF)c_{u,scr}(k)d_{u,c}\left(\lfloor k/SF\rfloor\right)\quad(2)$$

is the $k$-th subcarrier component with $P_u$ being the transmit power per code and $\lfloor a\rfloor$denoting the largest integer smaller than or equal to $a$.

Figure 2 illustrates the frame structure of the MC-CDMA signal. Each frame consists of $N_p$ OFDM pilot symbols and $N_d$ MC-CDMA data symbols; the OFDM pilot is allocated the same power (i.e., $(C/SF)P_u$) as the multi-code MC-CDMA data. The array weight updating is done by using OFDM pilot; however, ideal channel estimation is assumed (in practical systems, channel estimation is performed by using pilot).

## 2.2 Propagation Channel

The MC-CDMA signal is transmitted over a frequency-selective fading channel with $L$ independent propagation paths and is received by $M$ antennas. The $l$-th path gain and delay time associated with the $m$-th antenna are denoted by $h_{u,l,m}$ and $\tau_{u,l}$, respectively, with $E\left[\left|h_{u,l,m}\right|^2\right]=1/L$ for all $u$ and $m$ ($E[.]$ denotes the ensemble average operation). The received signal on the $m$-th antenna is given by

$$x_m(t)=\sum_{u=0}^{U-1}\sum_{l=0}^{L-1}s_u(t-\tau_{u,l})h_{u,l,m}+\eta_m(t)$$
$$\text{for } t=-N_g{\sim}N_c-1.\quad(3)$$

Here $\eta_m(t)$ is the noise having a variance of $2N_0/T_s$, where $N_0$ represents the single-sided additive white Gaussian noise (AWGN) power spectrum density and $T_s$ is the MC-CDMA signaling period including GI.

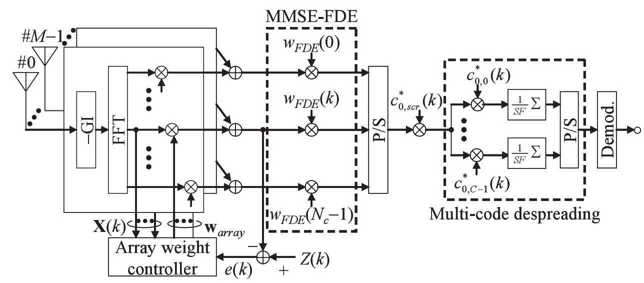


**Fig. 3** Receiver structure of the 0th user.

## 2.3 Received Signal

Without loss of generality, the $u$=0th user is assumed to be the desired user. Figure 3 illustrates the receiver structure for the 0th user. After the removal of the GI, $N_c$-point FFT is performed to decompose the received signal into $N_c$ subcarrier components. The $k$-th subcarrier component $X_m(k)$ is given by

$$\begin{aligned}X_m(k)&=\frac{1}{N_c}\sum_{k=0}^{N_c-1}x_m(t)\exp\left(-j2\pi k\frac{t}{N_c}\right)\\&=\sum_{u=0}^{U-1}S_u(k)H_{u,m}(k)+\Pi_m(k),\end{aligned}\quad(4)$$

where

$$\begin{cases}H_{u,m}(k)=\sum_{l=0}^{L-1}h_{u,l,m}\exp\left(-j2\pi k\frac{\tau_{u,l}}{N_c}\right)\\ \Pi_m(k)=\frac{1}{N_c}\sum_{t=0}^{N_c-1}\eta_m(t)\exp\left(-j2\pi k\frac{t}{N_c}\right)\end{cases}.\quad(5)$$

## 2.4 Adaptive Array and MMSE-FDE

Antenna array combining is done in the frequency-domain. The array combiner output $Y(k)$ for the $k$-th subcarrier is given by

$$\begin{aligned}Y(k)&=\boldsymbol{w}_{array}^T\boldsymbol{X}(k)=S_0(k)\boldsymbol{w}_{array}^T\boldsymbol{H}_0(k)\\&+\sum_{u=1}^{U-1}S_u(k)\boldsymbol{w}_{array}^T\boldsymbol{H}_u(k)+\boldsymbol{w}_{array}^T\boldsymbol{\Pi}(k),\end{aligned}\quad(6)$$

where $\boldsymbol{w}_{array}=[w_{array,0}, w_{array,1},\ldots,w_{array,M-1}]^T$ is the array weight vector, $\boldsymbol{X}(k)=[X_0(k), X_1(k),\ldots,X_{M-1}(k)]^T$, $\boldsymbol{H}_u(k)=[H_{u,0}(k), H_{u,1}(k),\ldots,H_{u,M-1}(k)]^T$, $\boldsymbol{\Pi}(k)=[\Pi_0(k), \Pi_1(k),\ldots,\Pi_{M-1}(k)]^T$. The array weight vector is the same for all subcarriers. Updating $\boldsymbol{w}_{array}$ is presented in Sect. 3.

After the array combining, MMSE-FDE is performed as

$$R(k)=w_{FDE}(k)Y(k)=\sum_{u=0}^{U-1}S_u(k)\tilde{H}_u(k)+\tilde{\Pi}(k),\quad(7)$$

where $w_{FDE}(k)$ is the equalization weight and

$$\begin{cases} \tilde{H}_u(k) = w_{FDE}(k)\boldsymbol{w}^T_{array}\boldsymbol{H}_u(k) \\ \tilde{\Pi}(k) = w_{FDE}(k)\boldsymbol{w}^T_{array}\boldsymbol{\Pi}(k) \end{cases}. \tag{8}$$

The mean square error (MSE) between the $k$-th subcarrier component $R(k)$ after FDE and the transmitted signal component $S_0(k)$ is written as

$$\begin{aligned} J_{FDE}(k) &= E\left[|R(k) - S_0(k)|^2\right] \\ &= 2\frac{C}{SF}|w_{FDE}(k)|^2\sum_{u=0}^{U-1}P_u\left|\boldsymbol{w}^T_{array}\boldsymbol{H}_u(k)\right|^2 \\ &\quad + |w_{FDE}(k)|^2\frac{2N_0}{T_s} + 2P_0\frac{C}{SF} \\ &\quad - 4P_0\frac{C}{SF}\mathrm{Re}\left[\left(w_{FDE}(k)\boldsymbol{w}^T_{array}\boldsymbol{H}_0(k)\right)^*\right], \end{aligned} \tag{9}$$

since

$$E\left[\left|\boldsymbol{w}^T_{array}\boldsymbol{\Pi}(k)\right|^2\right] = \frac{2N_0}{T_s} \tag{10}$$

from $\|\boldsymbol{w}_{array}\|^2 = 1$. The MMSE equalization weight is obtained from $\partial J_{FDE}(k)/\partial w_{FDE}(k) = 0$, where $\partial J_{FDE}(k)/\partial w_{FDE}(k)$ is given as

$$\frac{\partial J_{FDE}(k)}{\partial w_{FDE}(k)} = 4P_0\frac{C}{SF}\left(\begin{array}{l} w_{FDE}(k)\displaystyle\sum_{u=0}^{U-1}\frac{E_{s,u}}{E_{s,0}}\left|\boldsymbol{w}^T_{array}\boldsymbol{H}_u(k)\right|^2 \\ +\dfrac{N_0}{E_{s,0}}\dfrac{SF}{C} - \left(\boldsymbol{w}^T_{array}\boldsymbol{H}_0(k)\right)^* \end{array}\right) \tag{11}$$

with $E_{s,u} = P_uT_s$ being the symbol energy. The MMSE equalization weight is derived as

$$w_{FDE}(k) = \frac{\left(\boldsymbol{w}^T_{array}\boldsymbol{H}_0(k)\right)^*}{\displaystyle\sum_{u=0}^{U-1}\frac{E_{s,u}}{E_{s,0}}\left|\boldsymbol{w}^T_{array}\boldsymbol{H}_u(k)\right|^2 + \left(\frac{C}{SF}\frac{E_{s,0}}{N_0}\right)^{-1}}. \tag{12}$$

After MMSE-FDE, parallel-to-serial (P/S) conversion and multi-code despreading are performed to obtain

$$\hat{d}_{0,c}(i) = \frac{1}{SF}\sum_{k=iSF}^{(i+1)SF-1}R(k)\{c_{0,c}(k \bmod SF)c_{0,scr}(k)\}^* \tag{13}$$

for $i$=0~$(N_c/SF) - 1$ and $c$=0~$C - 1$. Finally, the data-demodulation is performed.

## 3. Frequency-Domain Array Weight Updating

### 3.1 MSE

The MMSE adaptive algorithm [10], which minimizes the MSE between the array output $Y(k)$ and the reference signal $Z(k)$, is used to determine the array weight vector. In the case of $Z(k) = p_0(k)$, the array weight has to not only suppress the interference but also perform coherent detection and therefore, the algorithm needs to track a time-selective fading. However, the BER performance degrades in a fast fading due to the tracking problem. Following the idea shown in [9], we use the desired signal component in Eq. (6) as $Z(k)$, which is given by

$$Z(k) = S_0(k)\boldsymbol{w}^T_{array}\boldsymbol{H}_0(k). \tag{14}$$

Therefore, the error signal $e(k)$ becomes

$$\begin{aligned} e(k) &= Z(k) - Y(k) \\ &= -\sum_{u=1}^{U-1}S_u(k)\boldsymbol{w}^T_{array}\boldsymbol{H}_u(k) - \boldsymbol{w}^T_{array}\boldsymbol{\Pi}(k). \end{aligned} \tag{15}$$

The MSE $E[|e(k)|^2]$ is given by

$$E\left[|e(k)|^2\right] = \boldsymbol{w}^H_{array}\boldsymbol{R}_{i+n}\boldsymbol{w}_{array}, \tag{16}$$

where the superscript $H$ denotes the Hermitian transposition and $R_{i+n}$ is the $M$-by-$M$ correlation matrix of the interference plus noise and is given by

$$\boldsymbol{R}_{i+n} = E\left[\sum_{u=1}^{U-1}(S_u(k)\boldsymbol{H}_u(k))^*(S_u(k)\boldsymbol{H}_u(k))^T\right] + \frac{2N_0}{T_s}\boldsymbol{I} \tag{17}$$

with $\boldsymbol{I}$ being an $M$-by-$M$ identity matrix. $\boldsymbol{w}_{array}$ is determined so that the MSE can be minimized. However, the solution includes $\boldsymbol{w}_{array} = \boldsymbol{0}$. To avoid this, we introduce the constraint

$$\|\boldsymbol{w}_{array}\|^2 = 1. \tag{18}$$

The phase and amplitude variations of the desired signal component, due to the fading, remain after the array combining. The fading compensation is a task of MMSE-FDE.

### 3.2 Optimum Array Weight

Under the constraint $\|\boldsymbol{w}_{array}\|^2 = 1$, we use the following cost function [10]

$$J_{array}(\boldsymbol{w}_{array}) = \boldsymbol{w}^H_{array}\boldsymbol{R}_{i+n}\boldsymbol{w}_{array} + \kappa\left(1 - \boldsymbol{w}^H_{array}\boldsymbol{w}_{array}\right), \tag{19}$$

where $\kappa$ denotes the complex Lagrange multiplier. Taking the derivative of $J_{array}(\boldsymbol{w}_{array})$ with respect to $\boldsymbol{w}_{array}$, we have

$$\frac{\partial J_{array}(\boldsymbol{w}_{array})}{\partial \boldsymbol{w}_{array}} = 2\boldsymbol{R}_{i+n}\boldsymbol{w}_{array} - 2\kappa\boldsymbol{w}_{array}. \tag{20}$$

By setting Eq. (20) to zero vector, we obtain

$$(\boldsymbol{R}_{i+n} - \kappa_{min}\boldsymbol{I})\,\boldsymbol{w}_{array} = \boldsymbol{0}. \tag{21}$$

Since $\boldsymbol{w}_{array} \neq 0$, $\boldsymbol{w}_{array}$ is one of the eigen vectors associated with eigen values $\kappa = \{\kappa_0, \kappa_1, \ldots, \kappa_{K-1}\}$, where $K$ is the rank of the matrix ($K \leq M$). Multiplying Eq. (21) by $\boldsymbol{w}^H_{array}$ gives

$$\boldsymbol{w}^H_{array}\boldsymbol{R}_{i+n}\boldsymbol{w}_{array} = \kappa\|\boldsymbol{w}_{array}\|^2 = \kappa. \tag{22}$$

Since our objective is to find $\boldsymbol{w}_{array}$ that minimizes $\boldsymbol{w}^H_{array}\boldsymbol{R}_{i+n}\boldsymbol{w}_{array}$, the optimum $\boldsymbol{w}_{array}$ is the eigen vector corresponding to the minimum eigen value $\kappa_{min}$. Hence, the optimum $\boldsymbol{w}_{array}$ is the one that satisfies

$$(\boldsymbol{R}_{i+n} - \kappa_{min}\boldsymbol{I})\,\boldsymbol{w}_{array} = \boldsymbol{0}. \tag{23}$$

### 3.3 Weight Updating Algorithm

The gradient vector $\nabla E\left[|e(k)|^2\right]$ [10] is given by

$$\nabla E\left[|e(k)|^2\right] = \frac{\partial E\left[|e(k)|^2\right]}{\partial \boldsymbol{w}_{array}} = 2\boldsymbol{R}_{i+n}\boldsymbol{w}_{array} = 2\boldsymbol{R}_{xx}\boldsymbol{w}_{array} - 2\boldsymbol{R}_{ss}\boldsymbol{w}_{array}, \tag{24}$$

where $R_{xx}$ and $R_{ss}$ are given by

$$\begin{cases} \boldsymbol{R}_{xx} = E\left[\boldsymbol{X}^*(k)\boldsymbol{X}^T(k)\right] \\ \boldsymbol{R}_{ss} = E\left[(S_0(k)\boldsymbol{H}_0(k))^* (S_0(k)\boldsymbol{H}_0(k))^T\right] \end{cases}. \tag{25}$$

Since there is no correlation between $S_0(k)$ and $S_u(k)$, and also between $S_0(k)$ and $\Pi_m(k)$, we have

$$\begin{aligned} &\boldsymbol{R}_{ss}\boldsymbol{w}_{array} \\ &= E\left[\left(\sum_{u=0}^{U-1} S_u(k)\boldsymbol{H}_u(k) + \boldsymbol{\Pi}(k)\right)^* S_0(k)\boldsymbol{w}_{array}^T\boldsymbol{H}_0(k)\right] \\ &= E\left[\boldsymbol{X}^*(k)Z(k)\right]. \end{aligned} \tag{26}$$

Therefore, Eq. (24) can be rewritten as

$$\begin{aligned} \nabla E\left[|e(k)|^2\right] &= 2\boldsymbol{R}_{xx}\boldsymbol{w}_{array} - 2\boldsymbol{R}_{ss}\boldsymbol{w}_{array} \\ &= 2E\left[\boldsymbol{X}^*(k)\boldsymbol{X}^T(k)\right]\boldsymbol{w}_{array} - 2E\left[\boldsymbol{X}^*(k)Z(k)\right] \\ &= E\left[2\boldsymbol{X}^*(k)\left(Y(k) - Z(k)\right)\right] \\ &= E\left[-2e(k)\boldsymbol{X}^*(k)\right]. \end{aligned} \tag{27}$$

Based on the steepest decent algorithm [10], we develop a stochastic adaptation algorithm. Removing the ensemble average operation from Eq. (27), we obtain the following algorithm similar to the well known NLMS algorithm:

$$\tilde{\boldsymbol{w}}_{array}^{(n+1)} = \boldsymbol{w}_{array}^{(n)} + 2\mu e(n \bmod N_c)\frac{\boldsymbol{X}^*(n \bmod N_c)}{\|\boldsymbol{X}(n \bmod N_c)\|^2} \tag{28}$$

for the $n$-th updating, where

$$\boldsymbol{w}_{array}^{(n+1)} = \tilde{\boldsymbol{w}}_{array}^{(n+1)} \Big/ \left\|\tilde{\boldsymbol{w}}_{array}^{(n+1)}\right\| \tag{29}$$

and $\mu$ is the step size. Equation (29) is necessary to satisfy the constraint $\left\|\boldsymbol{w}_{array}\right\|^2 = 1$. Since the same array weight vector is used for all the subcarriers, the weight updating, as many times as $N_c$, is possible within one MC-CDMA symbol duration.

## 4. Average Bit Error Rate

From Eqs. (2) and (7), Eq. (13) can be written as

$$\begin{aligned} \hat{d}_{0,c}(i) = &\frac{1}{SF}\sqrt{\frac{2P_0}{SF}}d_{0,c}(i)\sum_{k=iSF}^{(i+1)SF-1}\tilde{H}_0(k) \\ &+ \chi_{ICI}(i) + \chi_{MAI}(i) + \chi_{noise}(i), \end{aligned} \tag{30}$$

where the first term represents the desired signal component and the second, third, and fourth terms are the inter-code interference (ICI), residual MAI, and noise due to AWGN, respectively. $\chi_{ICI}(i)$, $\chi_{MAI}(i)$, and $\chi_{noise}(i)$ are given by

$$\begin{cases} \chi_{ICI}(i) = \frac{1}{SF}\sqrt{\frac{2P_0}{SF}}\sum_{k=iSF}^{(i+1)SF-1}\tilde{H}_0(k)c_{0,c}^*(k \bmod SF)c_{0,scr}^*(k) \\ \qquad \times \sum_{\substack{c'=0 \\ \neq c}}^{C-1} d_{0,c'}(i)c_{0,c'}(k \bmod SF)c_{0,scr}(k) \\ \chi_{MAI}(i) \\ \quad = \frac{1}{SF}\sum_{u=1}^{U-1}\sum_{k=iSF}^{(i+1)SF-1}\sqrt{\frac{2P_u}{SF}}\sum_{c=0}^{C-1} d_{u,c}(i)c_{u,c}(k \bmod SF) \\ \quad \times c_{u,scr}(k)\tilde{H}_u(k)c_{0,c}^*(k \bmod SF)c_{0,scr}^*(k) \\ \chi_{noise}(i) = \frac{1}{SF}\sum_{k=iSF}^{(i+1)SF-1}\tilde{\Pi}(k)c_{0,c}^*(k \bmod SF)c_{0,scr}^*(k) \end{cases}. \tag{31}$$

It can be understood from Eq. (30) that $\hat{d}_{0,c}(i)$ is a random variable with a mean $\frac{1}{SF}\sqrt{\frac{2P_0}{SF}}d_{0,c}(i)\sum_{k=iSF}^{(i+1)SF-1}\tilde{H}_0(k)$. Applying the Gaussian approximation of $\chi_{ICI}$ and $\chi_{MAI}$, the sum of $\chi_{ICI}$, $\chi_{MAI}$, and $\chi_{noise}$ can be treated as a new zero-mean complex-valued Gaussian variable $\chi$. The variance of $\chi$ is the sum of those of $\chi_{ICI}$, $\chi_{MAI}$, and $\chi_{noise}$:

$$2\sigma_\chi^2 = E\left[|\chi|^2\right] = 2\sigma_{\chi_{ICI}}^2 + 2\sigma_{\chi_{MAI}}^2 + 2\sigma_{\chi_{noise}}^2, \tag{32}$$

where, from Appendix,

$$\begin{cases} \sigma_{ICI}^2 = P_0\frac{C-1}{SF^3}\left(\sum_{k=iSF}^{(i+1)SF-1}\left|\tilde{H}_0(k)\right|^2 - \frac{1}{SF}\left|\sum_{k=iSF}^{(i+1)SF-1}\tilde{H}_0(k)\right|^2\right) \\ \sigma_{MAI}^2 = \frac{1}{SF^2}\sum_{u=1}^{U-1}P_u\frac{C}{SF}\sum_{k=iSF}^{(i+1)SF-1}\left|\tilde{H}_u(k)\right|^2 \\ \sigma_{noise}^2 = \frac{1}{SF^2}\frac{N_0}{T_s}\sum_{k=iSF}^{(i+1)SF-1}|w_{FDE}(k)|^2 \end{cases}. \tag{33}$$

Assuming quaternary phase shift keying (QPSK) data modulation, the conditional BER, for the given set of $\boldsymbol{\Gamma} = [E_{s,0}/N_0,\ E_{s,1}/N_0, \ldots, E_{s,U-1}/N_0]^T$ and $\boldsymbol{H} = [H_0(k), H_1(k), \ldots, H_{U-1}(k)]$, is given as [1]

$$P_b(\boldsymbol{\Gamma}, \boldsymbol{H}) = \frac{1}{2}erfc\left[\sqrt{\frac{1}{4}\gamma(\boldsymbol{\Gamma}, \boldsymbol{H})}\right], \tag{34}$$

where $erfc[x] = \int_x^\infty \exp(-t^2)dt$ is the complementary error function and $\gamma(\boldsymbol{\Gamma}, \boldsymbol{H})$ is the conditional signal-to-interference plus noise power ratio (SINR) defined as

$$\gamma(\boldsymbol{\Gamma},\boldsymbol{H}) = \frac{\dfrac{2P_0}{SF^3}\left|\displaystyle\sum_{k=iSF}^{(i+1)SF-1}\tilde{H}_0(k)\right|^2}{\sigma_\chi^2} = \frac{2\dfrac{1}{SF}\dfrac{E_{s,0}}{N_0}\left|\displaystyle\sum_{k=iSF}^{(i+1)SF-1}\tilde{H}_0(k)\right|^2}{\left(\begin{array}{l}\dfrac{C-1}{SF}\dfrac{E_{s,0}}{N_0}\left(\displaystyle\sum_{k=iSF}^{(i+1)SF-1}\left|\tilde{H}_0(k)\right|^2-\frac{1}{SF}\left|\sum_{k=iSF}^{(i+1)SF-1}\tilde{H}_0(k)\right|^2\right)\\ +\displaystyle\sum_{u=1}^{U-1}\frac{C}{SF}\frac{E_{s,u}}{N_0}\sum_{k=iSF}^{(i+1)SF-1}\left|\tilde{H}_u(k)\right|^2+\sum_{k=iSF}^{(i+1)SF-1}|w_{FDE}(k)|^2\end{array}\right)}. \quad (35)$$

The theoretical average BER can be numerically evaluated by averaging Eq. (34) over all possible $\boldsymbol{H}$.

## 5. Simulation and Numerical Results

Table 1 summarizes the computer simulation conditions. Multi-code MC-CDMA with equivalent spreading factor $SF_{eq}$ ($= SF/C$) = 1 is considered, which provides the same data rate as OFDM (note that $SF$=1 gives the OFDM signal). The OFDM pilot is generated using a binary random sequence. Channel coding and frequency-domain interleaving are not considered in this paper. We assume a frequency-selective block Rayleigh fading channel having a sample-spaced $L$=16-path uniform power delay profile (i.e., $E\left[\left|h_{u,l,m}\right|^2\right] = 1/L$ for all $u$ and $m$) and the $l$-th path delay time $\tau_{u,l,m} = l$ samples. The arrival angles of 16 paths are assumed to be uniformly distributed over the angle interval of $[\phi-\Delta, \phi+\Delta]$, where $\phi$ is called the nominal arrival angle and $\Delta$ is called the arrival angle spread. We will show the simulation and numerical results for the case of $U$=4 with the nominal arrival angles of $u$=0th, 1st, 2nd and 3rd users signals being 17°, 236°, 88° and 321°, respectively. The average received signal powers from all users are the same (i.e., the average received desired signal power-to-total interference power ratio (SIR) = −4.8 dB). The initial array weight is set as

$$w_{array,m}^{(0)} = \begin{cases} 1+j0, & m=0 \\ 0+j0, & m\neq 0 \end{cases}. \quad (36)$$

Besides the computer simulation of the signal transmission, the theoretical average BER is also evaluated numerically, using Monte-Carlo numerical computation method as follows. The set of path gains $\{h_{u,l,m};\ u=0\sim U-1,\ l=0\sim L-1,$ and $m=0\sim M-1\}$, is generated to obtain $\{H_u(k);\ k=0\sim N_c-1\}$, $\boldsymbol{w}_{array}$ and $\{w_{FDE}(k);\ k=0\sim N_c-1\}$, by using Eqs. (5), (23) and (12), respectively. The conditional BER for the given average received $E_s/N_0$ is computed by using Eq. (34). This is repeated a sufficient number of times to obtain the average BER.

Figure 4 shows the array weight vector convergence rate, measured by the average BER, with the step size $\mu$ as a parameter for OFDM case ($SF$=1). It is seen that the array weight vector $\boldsymbol{w}_{array}$ converges within one OFDM symbol duration for $\mu$=1/8 and 1/32, since the proposed adaptive array is able to update the array weight vector as many times as the number of subcarriers. Figure 5 shows the beam pattern generated after the array weight has converged. It is seen that the nulls are directed to the interfering users. As the step size $\mu$ increases, a faster convergence can be seen, but the BER after the weight vector has converged becomes higher (see Fig. 4). In the following simulation, we use $\mu$=1/32.

Figure 6 shows the convergence rate with $SF$ as a parameter for the case of equivalent spreading factor $SF_{eq}$=1. As $SF$ increases, the BER after the weight has converged becomes smaller. This is because the frequency diversity effect increases as $SF$ increases. Also seen from Fig. 6 is that the adaptation algorithm developed in Sect 3.3 gives an

**Table 1** Simulation and numerical condition.

| | | |
|---|---|---|
| Transmitter | Modulation | QPSK |
| | No. of subcarriers | $N_c$=256 |
| | Guard interval | $N_g$=32 |
| | Orthogonal code | Walsh-Hadamard code |
| | Scramble code | Long PN code |
| Channel | No. of users | $U$=4 |
| | Fading | Frequency-selective block Rayleigh fading channel |
| | Power delay profile | $L$=16-path uniform power delay profile |
| | Time delay | $\tau_{u,m,l}$=$l$, $l$=0~$L$−1 |
| Receiver | No. of antennas | $M$=4 (Linear array) |
| | Antenna interval | $d$=0.5$\lambda$ |
| | Channel estimation | Ideal |

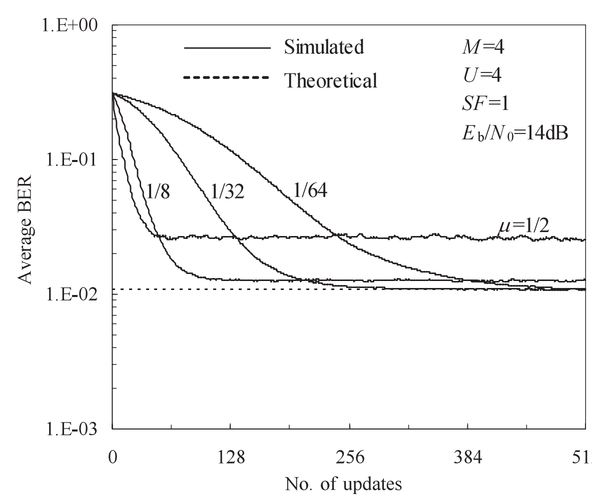


**Fig. 4** Impact of step size $\mu$.

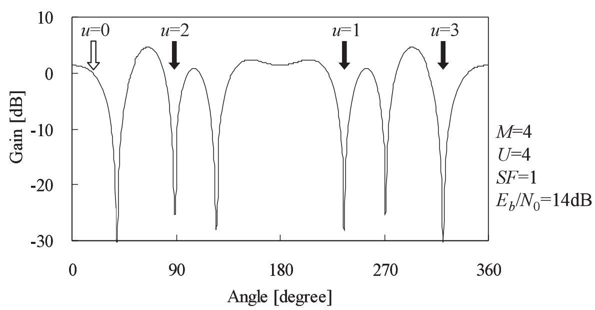


**Fig. 5** Generated beam pattern.

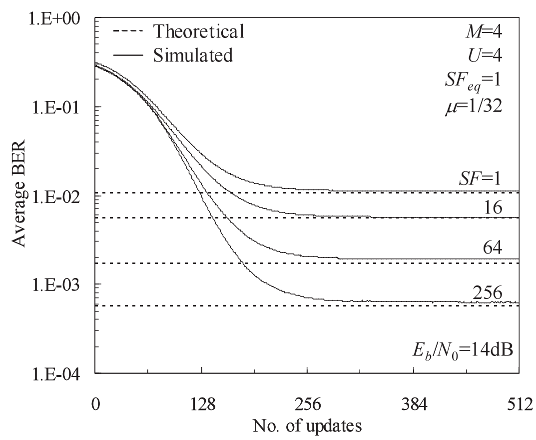


**Fig. 6** Convergence rate when $SF_{eq}$=1.

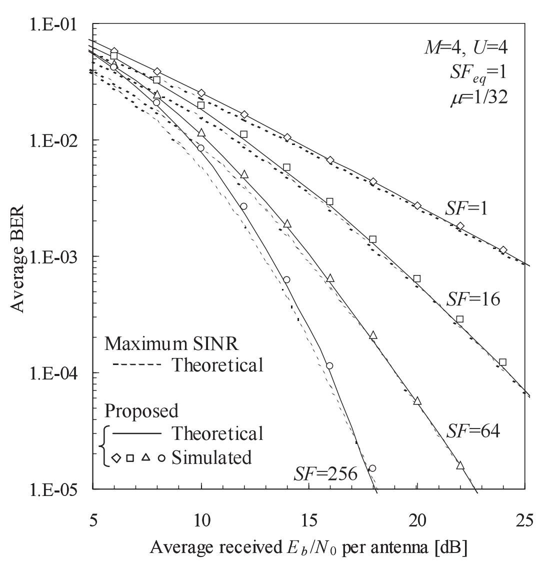


**Fig. 7** BER performance when $SF_{eq}$=1.

array weight close to the theoretically predicted one given by Eq. (23).

Figure 7 plots the average BER performance obtained after weight updating 512 times (i.e., after 2 OFDM symbols duration) with $SF$ as a parameter for the case of $SF_{eq}(=C/SF)=1$. For comparison, the theoretical BER of Wiener solution (maximum SINR) case is plotted. It is seen that as $SF$ increases, the BER performance improves since a larger frequency diversity effect is obtained. In a high $E_b/N_0$ region, the BER of the proposed array is almost close to the Wiener solution case. On the other hand, although the proposed array slightly degrades from the Wiener solution case in a low $E_b/N_0$ region, it provides a BER performance close to the Wiener solution case. We have also examined the BER performance using antenna diversity reception using maximal ratio combining (the results are not shown here) and found that a large BER floor of around BER=0.1 appears since the antenna diversity reception cannot sufficiently suppress the MAI.

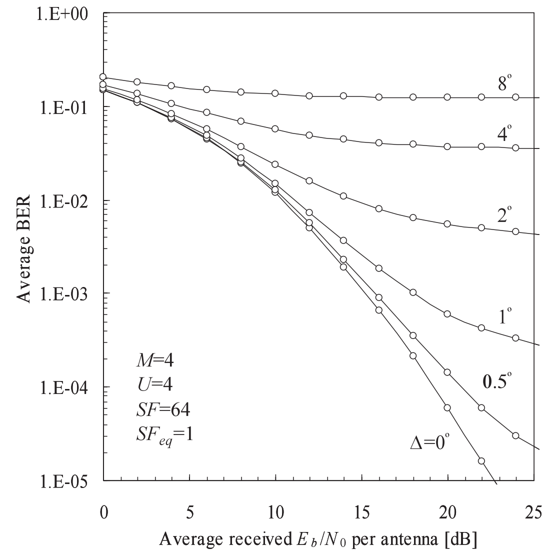


**Fig. 8** Impact of arrival angle spread Δ.

Figure 8 plots the average BER performance obtained after weight updating 512 times with the arrival angle spread Δ as a parameter for the case of $SF_{eq}$=1. The proposed adaptive antenna array is designed to minimize the average interference power and therefore, if $L$ paths arrive from different directions, different paths look like different users; hence, the equivalent number $U_e$ of users is given by the number of users times that of paths, i.e., $U_e = L \times U$. Therefore, even if $M = U = 4$, as Δ increases, the BER floor appears and the achievable BER performance degrades due to the increase of the BER floor. As a consequence, the proposed adaptive antenna array is effective only when Δ is very small; this happens if the base station antenna height is high enough so that there is no obstacle which blocks the interfering signals. This is a limitation of the proposed adaptive antenna array (Note that the proposed adaptive antenna array is based on the average interference power minimization criterion and hence, can only suppress the interference power; even when $U_e < M$, it cannot increase the desired signal power unlike the adaptive antenna array using a different array weight vector on a different subcarrier).

## 6. Conclusion

In this paper, we proposed a frequency-domain adaptive antenna array for multi-code MC-CDMA uplink transmission. In the proposed array, the same array weight is used for all subcarriers and hence the weight update can be done as many times as the number of subcarriers within one MC-CDMA symbol duration. Therefore, a very fast weight convergence is achieved although a simple NLMS algorithm is used. The MMSE-FDE weight taking into account the residual MAI after array combining was derived and the average BER performance was theoretically analyzed. The effectiveness of the proposed array was confirmed by both computer simulation and numerical evaluation.

In this paper, we assumed ideal channel estimation. However, the channel estimation accuracy may degrade in a multi-user environment, thereby degrading the antenna beam forming. There are many literatures concerning channel estimation, e.g., [11]–[13]. The impact of channel estimation errors on the proposed adaptive antenna array is left as an important future work.

### References


[1] J.G. Proakis, Digital communications, 3rd ed., McGraw Hill, 1995.
[2] S. Hara and R. Prasad, Multicarrier Techniques for 4G Mobile Communications, Artech House, 2003.
[3] N. Maeda, H. Atarashi, S. Abeta, and M. Sawahashi, "Antenna diversity reception appropriate for MMSE combining in frequency domain for forward link OFCDM packet wireless access," IEICE Trans. Commun., vol.E85-B, no.10, pp.1966–1977, Oct. 2002.
[4] H. Atarashi, S. Abeta, and M. Sawahashi, "Variable spreading factor-orthogonal frequency and code division multiplexing (VSF-OFCDM) for broadband packet wireless access," IEICE Trans. Commun., vol.E86-B, no.1, pp.291–299, Jan. 2003.
[5] J.C. Liberti and T.S. Rappaport, Smart Antennas for Wireless Communications: IS-95 & 3rd Generation CDMA Applications, Prentice Hall, 1999.
[6] Y. Li and N.R. Sollenberger, "Adaptive antenna arrays for OFDM systems with cochannel interference," IEEE Trans. Commun., vol.47, no.2, pp.217–229, Feb. 1999.
[7] T. Fujii and M. Nakagawa, "Unicast and broadcast packet sharing method for OFDM multi-base station system with array antenna on mobile terminal," IEICE Trans. Commun., vol.E85-B, no.2, pp.514–522, Feb. 2002.
[8] M. Budsabathon, Y. Hara, and S. Hara, "Optimum beam-forming for pre-FFT OFDM adaptive antenna array," IEEE Trans. Veh. Technol., vol.53, no.4, pp.945–955, July 2004.
[9] S. Tanaka, M. Sawahashi, and F. Adachi, "Pilot symbol-assisted decision-direct coherent adaptive array diversity for DS-CDMA mobile radio reverse link," IEICE Trans. Commun., vol.E80-A, no.12, pp.2445–2454, Dec. 1997.
[10] S. Haykin, Adaptive Filter Theory, 4th ed., Prentice Hall, 2001.
[11] F.W. Vook and T.A. Thomas, "MMSE multi-user channel estimation for broadband wireless communications," Proc. IEEE GLOBECOM'01, vol.1, pp.470–474, Nov. 2001.
[12] Y. Ogawa, K. Nishio, T. Nishimura, and T. Ohgane, "Channel estimation and signal detection for space division multiplexing in a MIMO-OFDM system," IEICE Trans. Commun., vol.E88-B, no.1, pp.10–18, Jan. 2005.
[13] G.L. Stuber, J.R. Barry, S.W. McLaughlin, L. Ye, M.A. Ingram, and T.G. Pratt, "Broadband MIMO-OFDM wireless communications," Proc. IEEE, vol.9, no.2, pp.271–294, Feb. 2004.
[14] W. Davenport and W. Root, An introduction to the theory of random signals and noise, McGraw Hill, 1958.


## Appendix: Derivation of $\sigma^2_{ICI}$, $\sigma^2_{MAI}$, and $\sigma^2_{noise}$

For simplicity, we denote $c_{u,c}(k \bmod SF)c_{u,scr}(k)$ by $c_{u,c}(k)$. The ICI, residual MAI, and noise can be rewritten as

$$\begin{cases} \chi_{ICI}(i) = \dfrac{1}{SF}\sqrt{\dfrac{2P_0}{SF}} \displaystyle\sum_{k=iSF}^{(i+1)SF-1} \tilde{H}_0(k)c^*_{0,c}(k) \sum_{\substack{c'=0\\ \neq c}}^{C-1} d_{0,c'}(i)c_{0,c'}(k) \\ \chi_{MAI}(i) = \dfrac{1}{SF}\displaystyle\sum_{u=1}^{U-1}\sum_{k=iSF}^{(i+1)SF-1}\sqrt{\dfrac{2P_u}{SF}} \\ \qquad \displaystyle\sum_{c=0}^{C-1} d_{u,c}(i)c_{u,c}(k)\tilde{H}_u(k)c^*_{0,c}(k) \\ \chi_{noise}(i) = \dfrac{1}{SF}\displaystyle\sum_{k=iSF}^{(i+1)SF-1} \tilde{\Pi}(k)c^*_{0,c}(k) \end{cases} \quad (\mathrm{A}\cdot 1)$$

Letting

$$\bar{H}_u(k) = \frac{1}{SF}\sum_{k=iSF}^{(i+1)SF-1} \tilde{H}_u(k), \quad (\mathrm{A}\cdot 2)$$

we have $\tilde{H}_u(k) = \left\{\tilde{H}_u(k) - \bar{H}_u(k)\right\} + \bar{H}_u(k)$. Therefore, $\chi_{ICI}(i)$ can be rewritten as

$$\chi_{ICI}(i) = \frac{1}{SF}\sqrt{\frac{2P_0}{SF}}\sum_{k=iSF}^{(i+1)SF-1}\sum_{\substack{c'=0\\ \neq c}}^{C-1}\left\{\tilde{H}_0(k) - \bar{H}_0(k)\right\} d_{0,c'}(i)c_{0,c'}(k)c^*_{0,c}(k), \quad (\mathrm{A}\cdot 3)$$

since

$$\sum_{k=nSF}^{(n+1)SF-1} c_{u,c'}(k)c^*_{u,c}(k) = 0, \quad \text{if } c \neq c'. \quad (\mathrm{A}\cdot 4)$$

We have

$$\begin{aligned} \sigma^2_{ICI} &= \frac{1}{2}E\left[|\chi_{ICI}|^2\right] \\ &= \frac{P_0}{SF^3}\sum_{k=iSF}^{(i+1)SF-1}\sum_{k'=iSF}^{(i+1)SF-1}\sum_{\substack{c'=0\\ \neq c}}^{C-1}\sum_{\substack{c''=0\\ \neq c}}^{C-1} \\ &\quad \left(\tilde{H}_0(k) - \bar{H}_0(k)\right)\left(\tilde{H}_0(k') - \bar{H}_0(k')\right)^* \\ &\quad \times E\left[d_{0,c'}(i)d^*_{0,c''}(i)c_{0,c'}(k)c^*_{0,c}(k)c^*_{0,c''}(k')c_{0,c}(k')\right] \end{aligned} \quad (\mathrm{A}\cdot 5)$$

Since $E\left[d_{0,c'}(i)d^*_{0,c''}(i)\right] = 0$ if $c' \neq c''$, we have

$$\begin{aligned} \sigma^2_{ICI} &= \frac{P_0}{SF^3}\sum_{k=iSF}^{(i+1)SF-1}\sum_{\substack{c'=0\\ \neq c}}^{C-1}\left|\tilde{H}_0(k) - \bar{H}_0(k)\right|^2 \\ &\quad + \frac{P_0}{SF^3}\sum_{k=iSF}^{(i+1)SF-1}\sum_{k'=iSF}^{(i+1)SF-1}\sum_{\substack{c'=0\\ \neq c,c''}}^{C-1}\sum_{\substack{c''=0\\ \neq c,c'}}^{C-1} \\ &\quad \times\left(\tilde{H}_0(k) - \bar{H}_0(k)\right)\left(\tilde{H}_0(k') - \bar{H}_0(k')\right)^* \\ &\quad \times E\left[c_{0,c'}(k)c^*_{0,c}(k)c^*_{0,c''}(k')c_{0,c}(k')\right], \end{aligned} \quad (\mathrm{A}\cdot 6)$$

Applying the law of large numbers [14], the second term of Eq. (A· 6) is zero. Hence, we obtain

$$\sigma_{ICI}^2 = P_0 \frac{C-1}{SF^3}\left(\sum_{k=iSF}^{(i+1)SF-1}\left|\tilde{H}_0(k)\right|^2 - \frac{1}{SF}\left|\sum_{k=iSF}^{(i+1)SF-1}\tilde{H}_0(k)\right|^2\right). \tag{A· 7}$$

Next, $\sigma_{MAI}^2$ is given by

$$\begin{aligned}\sigma_{MAI}^2 &= \frac{1}{2}E\left[|\chi_{MAI}|^2\right]\\ &= \sum_{u=1}^{U-1}\sum_{u'=1}^{U-1}\frac{P_u}{SF^3}\sum_{k=iSF}^{(i+1)SF-1}\sum_{k'=iSF}^{(i+1)SF-1}\sum_{c=0}^{C-1}\sum_{c'=0}^{C-1}\tilde{H}_u(k)\tilde{H}_{u'}^*(k')\\ &\times E\left[d_{u,c}(i)d_{u',c'}^*(i)c_{u,c}(k)c_{u',c'}^*(k')c_{0,c}^*(k)c_{0,c'}(k')\right]\\ &= \sum_{u=1}^{U-1}P_u\frac{C}{SF^3}\sum_{k=iSF}^{(i+1)SF-1}\left|\tilde{H}_u(k)\right|^2.\end{aligned} \tag{A· 8}$$

Finally, $\sigma_{noise}^2$ is given by

$$\begin{aligned}\sigma_{noise}^2 &= \frac{1}{2}E\left[|\chi_{noise}|^2\right]\\ &= \frac{1}{2}\frac{1}{SF^2}\sum_{k=iSF}^{(i+1)SF-1}|w_{FDE}(k)|^2\, E\left[\left|\boldsymbol{w}_{array}^T\boldsymbol{\Pi}(k)\right|^2\right]\\ &= \frac{1}{SF^2}\frac{N_0}{T_s}\sum_{k=iSF}^{(i+1)SF-1}|w_{FDE}(k)|^2.\end{aligned} \tag{A· 9}$$

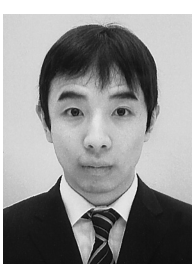

**Osamu Nakamura** received his B.S. and M.S. degrees in communications engineering from the Dept. of Electrical and Communications Engineering, Tohoku University, Sendai, Japan, in 2004 and 2006, respectively. Since April 2006, he has been with Sharp Corporation, where he is involved with Advanced Telecommunication Laboratory. He is engaged in research for Beyond 3G mobile communications systems.

**Shinsuke Takaoka** received his B.S., M.S. and Ph.D. degrees in communications engineering from Tohoku University, Sendai, Japan, in 2001, 2003 and 2006 respectively. Currently, he is with Matsushita Electric Industrial Co., Ltd. His research interests include digital signal transmission techniques, especially for mobile communication systems.

**Eisuke Kudoh** received the B.S. and M.S. degrees in physics and Ph.D. degree in electronic engineering from Tohoku University, Sendai, Japan, in 1986, 1988, and 2001, respectively. In April 1988, he joined the NTT Radio Communication Systems Laboratories, Kanagawa, Japan. He was engaged in research on digital mobile and personal communication systems including CDMA systems and error control schemes, etc. Since October 2001, he has been with Tohoku University, Sendai, Japan, where he is an Associate Professor of Electrical and Communication Engineering at Graduate School of Engineering. His research interests are in wireless network, wireless packet transmission, etc.

**Fumiyuki Adachi** received his B.S. and Dr. Eng. degrees in electrical engineering from Tohoku University, Sendai, Japan, in 1973 and 1984, respectively. In April 1973, he joined the Electrical Communications Laboratories of Nippon Telegraph & Telephone Corporation (now NTT) and conducted various types of research related to digital cellular mobile communications. From July 1992 to December 1999, he was with NTT Mobile Communications Network, Inc. (now NTT DoCoMo, Inc.), where he led a research group on wideband/broadband CDMA wireless access for IMT-2000 and beyond. Since January 2000, he has been with Tohoku University, Sendai, Japan, where he is a Professor of Electrical and Communication Engineering at Graduate School of Engineering. His research interests are in CDMA and TDMA wireless access techniques, CDMA spreading code design, Rake receiver, transmit/receive antenna diversity, adaptive antenna array, bandwidth-efficient digital modulation, and channel coding, with particular application to broadband wireless communications systems. From October 1984 to September 1985, he was a United Kingdom SERC Visiting Research Fellow in the Department of Electrical Engineering and Electronics at Liverpool University. From April 1997 to March 2000, he was a visiting Professor at Nara Institute of Science and Technology, Japan. He has written chapters of three books: Y. Okumura and M. Shinji Eds., "Fundamentals of mobile communications" published in Japanese by IEICE, 1986; M. Shinji, Ed., "Mobile communications" published in Japanese by Maruzen Publishing Co., 1989; and M. Kuwabara ed., "Digital mobile communications" published in Japanese by Kagaku Shinbun-sha, 1992. He was a co-recipient of the IEICE Transactions best paper of the year award 1996 and again 1998. He is an IEEE Fellow and was a co-recipient of the IEEE Vehicular Technology Transactions best paper of the year award 1980 and again 1990 and also a recipient of Avant Garde award 2000.